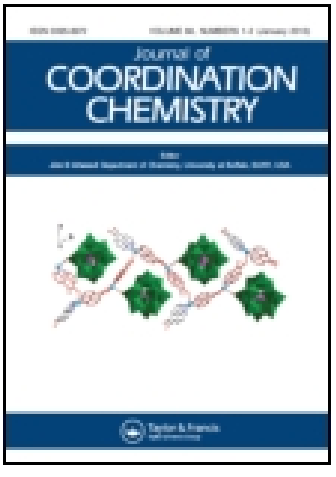

Journal of Coordination Chemistry
Publication details, including instructions for authors and subscription information:
http://www.tandfonline.com/loi/gcoo20

Construction of two interpenetrating coordination networks based on 4,4′-bis(1H-imidazol-1-yl-methyl)biphenyl and effect of carboxylic acids

Ying-Hui Yu[ab], Bo Wen[b], Han-Zhong Zhang[b], Guang-Feng Hou[a], Jin-Sheng Gao[ab] & Peng-Fei Yan[b]

[a] Engineering Research Center of Pesticide of Heilongjiang University, Heilongjiang University, Harbin, China

[b] School of Chemistry and Materials Science, Heilongjiang University, Harbin, China

Accepted author version posted online: 26 Feb 2014.Published online: 19 Mar 2014.

To cite this article: Ying-Hui Yu, Bo Wen, Han-Zhong Zhang, Guang-Feng Hou, Jin-Sheng Gao & Peng-Fei Yan (2014) Construction of two interpenetrating coordination networks based on 4,4′-bis(1H-imidazol-1-yl-methyl)biphenyl and effect of carboxylic acids, Journal of Coordination Chemistry, 67:4, 588-596, DOI: 10.1080/00958972.2014.895824

To link to this article: http://dx.doi.org/10.1080/00958972.2014.895824

Journal of Coordination Chemistry, 2014
Vol. 67, No. 4, 588–596, http://dx.doi.org/10.1080/00958972.2014.895824

Construction of two interpenetrating coordination networks based on 4,4′-bis(1H-imidazol-1-yl-methyl)biphenyl and effect of carboxylic acids

YING-HUI YU†‡, BO WEN‡, HAN-ZHONG ZHANG‡, GUANG-FENG HOU†, JIN-SHENG GAO*†‡ and PENG-FEI YAN‡

†Engineering Research Center of Pesticide of Heilongjiang University, Heilongjiang University, Harbin, China
‡School of Chemistry and Materials Science, Heilongjiang University, Harbin, China

(*Received 30 August 2013; accepted 16 December 2013*)

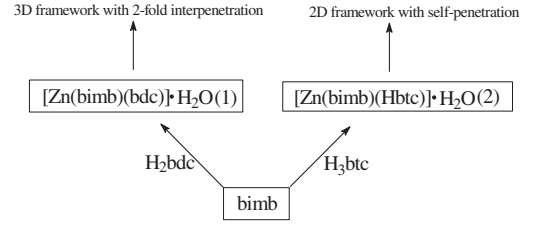

Effect of H_2bdc and H_3btc as different mixed ligand on the structures of zinc coordination polymers based on bimb

To investigate the construction of interpenetrating coordination networks and the effect of ligands, [Zn(bimb)(bdc)]·H_2O (**1**) and [Zn(bimb)(Hbtc)]·H_2O (**2**) [bimb = 4,4′-bis(1H-imidazol-1-yl-methyl) biphenyl; H_2bdc = 1,2-benzenedicarboxylic acid; H_3btc = 1,3,5-benzenetricarboxylic acid] were hydrothermally synthesized and characterized by elemental analysis, IR spectra, Powder X-ray diffraction, and thermogravimetric analysis. Complex **1** shows a 3-D **uoc** type topology with twofold interpenetration. However, **2** exhibits a different 2-D self-penetrating network owing to hydrogen bonds of Hbtc between the two interpenetrating **sql** sheets, indicating that different carboxylic ligands could affect the interpenetration structures. Photoluminescence of bimb and the two complexes are also studied.

Keywords: Crystal structure; Metal-organic frameworks; Interpenetration; Self-penetration; Photoluminescence property

1. Introduction

The design and synthesis of metal-organic frameworks (MOFs) with interesting structures and properties have been an area of rapid growth for potential applications as functional

*Corresponding author. Email: gaojins@hlju.edu.cn

materials and interesting molecular topologies [1]. Many coordination networks are fascinating for different entanglements. Interpenetrating networks are the most studied entangled arrays, arising from large free voids in a single network. Batten and Robson restricted the scope of interpenetrating structures wherein the building blocks within individual infinite networks or chains are linked through either metal-to-ligand bonds or hydrogen bonds [2]. When the individual networks are sufficiently open, interpenetration can occur [3]. Self-penetrating frameworks represent a subclass of interpenetration, featuring one of the "shortest rings" being catenated by other "shortest rings" of the same net [4].

Although many interesting coordination networks have been reported, it is still a challenge to predict the structure. The degree of interpenetration is strongly affected by the length of the spacer ligand. There are, however, other factors that are related to interpenetration, such as bulkiness of the ligands and the counterions, the number and type of solvated molecules, π–π interactions between the aromatic bridging ligands, and coordination geometries [5].

Flexible N-donors such as 1,4-bis(imidazole-l-ylmethyl)benzene (bix) have been widely adopted in the construction of MOFs with diverse topologies [6], many of which show different entanglement [7]. Compared with bix, 4,4′-bis(1H-imidazol-1-yl-methyl)biphenyl (bimb) is a longer spacer ligand with more flexibility that can adopt different conformations, based on which 1-, 2-, and 3-D structures were obtained [8]. Considering its long and flexible biphenyl group is favorable for formation of frameworks with large cavities, bimb is adopted in our study for the construction of high-dimensional interpenetrating structures.

Herein, we investigate the influence of different carboxylic acids on the formation of interpenetration structures based on bimb. We report two coordination complexes, [Zn(bimb)(bdc)]·H_2O (**1**) and [Zn(bimb)(Hbtc)]·H_2O (**2**), based on 1,2-benzenedicarboxylic acid (H_2bdc) and 1,3,5-benzenetricarboxylic acid (H_3btc), respectively. Complex **1** shows a 3-D network with twofold interpenetrating **uoc** net, hydrothermally synthesized by reacting zinc nitrate with bimb and H_2bdc. Complex **2** was obtained following the same procedure as for **1** except that H_3btc was used instead of H_2bdc. However, **2** exhibits a different 2-D self-penetration network. The structures of bimb, H_2bdc, and H_3btc are shown in scheme 1. The thermal stabilities and photoluminescence of the two complexes have also been described.

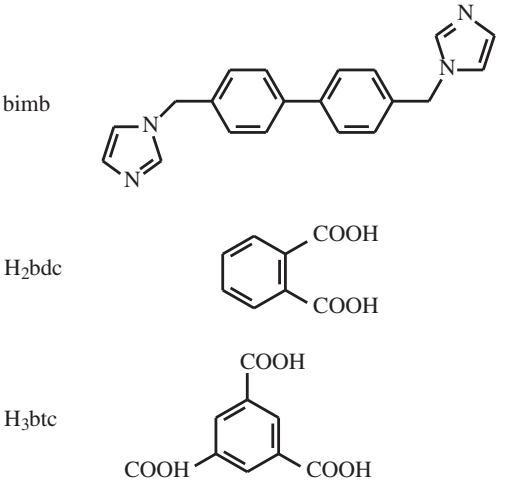

Scheme 1. Structures of bimb, H_2bdc and H_3btc.

2. Experimental setup

2.1. *Materials and measurements*

Zinc nitrate, ethanol, imidazole, and 1,2-benzenedicarboxylic acid are from Kermel and 4,4′-bis(chloromethyl)-1,1′-biphenyl from J&K Chemicals. All chemicals purchased are of reagent grade and used as received.

Elemental analyses for C, H, and N were carried out on a Vario EL III elemental analyzer. IR spectrum was recorded on a Bruker tensor 27 FT-IR spectrophotometer from 4000 to 400 cm^{-1} using KBr pellets. Photoluminescence spectra were taken on a Perkin Elmer Corporation Model Fluorescence Spectrometer LS 55 PL. Photoluminescence spectra were performed on solid samples after the crystals were crushed and put between quartz plates. Thermogravimetric analyses were carried out with a Perkin Elmer DTA-1700 with a heating rate of 10 °C min^{-1} from 25 to 800 °C. Powder X-ray diffraction (PXRD) measurement, from 2θ 5° to 50°, was performed on a Rigaku D/Max−IIIB with X-ray diffractometer Cu Kα ($\lambda = 1.5406$ Å) radiation (40 kV and 200 mA) and Ni filter.

2.2. *Synthesis*

2.2.1. Synthesis of [Zn(bimb)(bdc)]·H_2O (1). 4,4′-Bis(1H-imidazol-1-yl-methyl)biphenyl (bimb) was prepared following the literature procedure [9]. $Zn(NO_3)_2 \cdot 6H_2O$ (0.12 g, 0.40 mM), bimb (0.13 g, 0.40 mM), H_2bdc (0.07 g, 0.40 mM), H_2O (4 mL), and ethanol (4 mL) were stirred for 10 min in air, then the pH was adjusted to 6–7 by 1 M NaOH solution before the mixture was transferred and sealed in a 20 mL teflon-lined stainless autoclave, which was heated at 140 °C for 3 days and then cooled to room temperature. About 0.119 g colorless block crystals were filtered and washed with distilled water and ethanol (53% yield based on Zn^{II} cation). Elemental analysis: Calcd for $C_{28}H_{24}N_4O_5Zn$ (561.88): C, 59.85%; H, 4.31%; N, 9.97%. Found: C, 59.92%; H, 4.39%; N, 10.01%. IR (KBr, cm^{-1}): 3545 (w), 3447 (w), 3123 (w), 1695 (w), 1581 (m), 1498 (m), 1448 (m), 1398 (m), 1338 (w), 1280 (m), 1230 (m), 1187 (w), 1099 (s), 1005 (w), 952 (m), 827 (s), 750(s), 691 (w), 627 (w), 502 (w).

2.2.2. Synthesis of [Zn(bimb)(Hbtc)]·H_2O (2). The preparation of **2** was similar to that of **1** except that H_3tbc (0.08 g, 0.40 mM) instead of H_2bdc was used. About 0.114 g colorless block crystals were obtained after filtration and washed with distilled water and ethanol (47% yield based on Zn^{II}). Elemental analysis: Calcd for $C_{29}H_{24}N_4O_7Zn$ (605.91): C, 57.49%; H, 3.99%; N, 9.25%. Found: C, 57.31%; H, 3.72%; N, 9.39%. IR (KBr, cm^{-1}): 3133 (w), 1715 (s), 1617 (s), 1577 (m), 1357 (s), 1230 (m), 1166 (m), 1093 (m), 951 (w), 830 (w), 798 (w), 779 (s), 654 (m).

2.3. *X-ray crystallography*

Single-crystal X-ray diffraction data for **1** and **2** were collected on a Rigaku R-AXIS RAPID imaging plate diffractometer with graphite-monochromated Mo-Kα radiation ($\lambda =$ 0.71073 Å) at 291 K. Empirical absorption corrections based on equivalent reflections were applied. The structures of **1** and **2** were solved by direct methods and refined by full-matrix least-squares method on F^2 using the *SHELXS-97* crystallographic software package [10].

Table 1. Crystal data and structure refinements for **1** and **2**.

	1	**2**
Empirical formula	$C_{28}H_{24}N_4O_5Zn$	$C_{29}H_{24}N_4O_7Zn$
Fw	561.88	605.91
Crystal system	Tetragonal	Monoclinic
Space group	$I4_1/a$	$P2_1/c$
a (Å)	19.891(3)	11.138(2)
b (Å)	19.891(2)	19.068(4)
c (Å)	26.227(5)	16.848(5)
α (°)	90	90
β (°)	90	130.143(19)
γ (°)	90	90
V (Å^3)	10,377(3)	2735.3(11)
Z	16	4
D_{Calcd} (mg m^{-3})	1.439	1.471
μ (mm^{-1})	0.993	0.953
F (0 0 0)	4640	1248
Collected/unique	48,423/5924	24,938/6134
R(int)	0.0887	0.0497
GOF on F^2	1.035	1.027
R_1[a] [$I > 2\sigma(I)$]; wR_2[b] [$I > \sigma(I)$]	0.0436; 0.0919	0.0588; 0.1676
R_1[a] (all); wR_2[b] (all)	0.0837; 0.1051	0.0849; 0.1898

[a]$R_1 = \Sigma||Fo| - |Fc||/\Sigma|Fo|$.
[b]$wR_2 = \{\Sigma[w(F_o^2 - F_c^2)^2/\Sigma w(F_o^2)^2]\}^{1/2}$.

Table 2. Selected bond lengths [Å] and angles [°] of **1** and **2**.

Complex **1**			
Zn(1)–O(4)	1.9954(19)	Zn(1)–N(3)	2.006(2)
Zn(1)–N(1)	1.996(2)	Zn(1)–O(1)	1.9970(19)
O(4)–Zn(1)–N(1)	105.11(9)	O(4)–Zn(1)–N(3)	104.20(9)
O(4)–Zn(1)–O(1)	107.11(8)	N(1)–Zn(1)–N(3)	125.05(10)
N(1)–Zn(1)–O(1)	108.51(9)	O(1)–Zn(1)–N(3)	105.71(9)
Complex **2**			
N(1)–Zn(1)	2.021(4)	O(1)–Zn(1)	1.920(3)
N(3)–Zn(1)	2.022(3)	O(5)–Zn(1)	1.930(3)
O(1)–Zn(1)–O(5)	118.62(14)	O(1)–Zn(1)–N(1)	115.05(13)
O(5)–Zn(1)–N(1)	102.27(13)	O(1)–Zn(1)–N(3)	105.40(13)
O(5)–Zn(1)–N(3)	112.41(13)	N(1)–Zn(1)–N(3)	102.06(14)

All non-hydrogen atoms were refined anisotropically. Hydrogens of bimb and bdc were placed in calculated positions and treated as riding on their parent. In **1**, hydrogens of water were located in the difference Fourier map and refined as riding on their parent oxygen. However, in **2**, hydrogens of water were not added. The crystal parameters, data collection, and refinement results for **1** and **2** are summarized in table 1. Selected bond lengths and angles are listed in table 2. Crystallography data have been deposited to the Cambridge Crystallography Data Center with deposition numbers CCDC: 953109 and 953110.

3. Results and discussion

3.1. *Structure description*

Single-crystal X-ray diffraction analysis shows that the asymmetric unit of **1** contains two half bimb molecules, one Zn^{II}, one bdc anion, and one lattice water [figure 1(a)]. Zn^{II} is

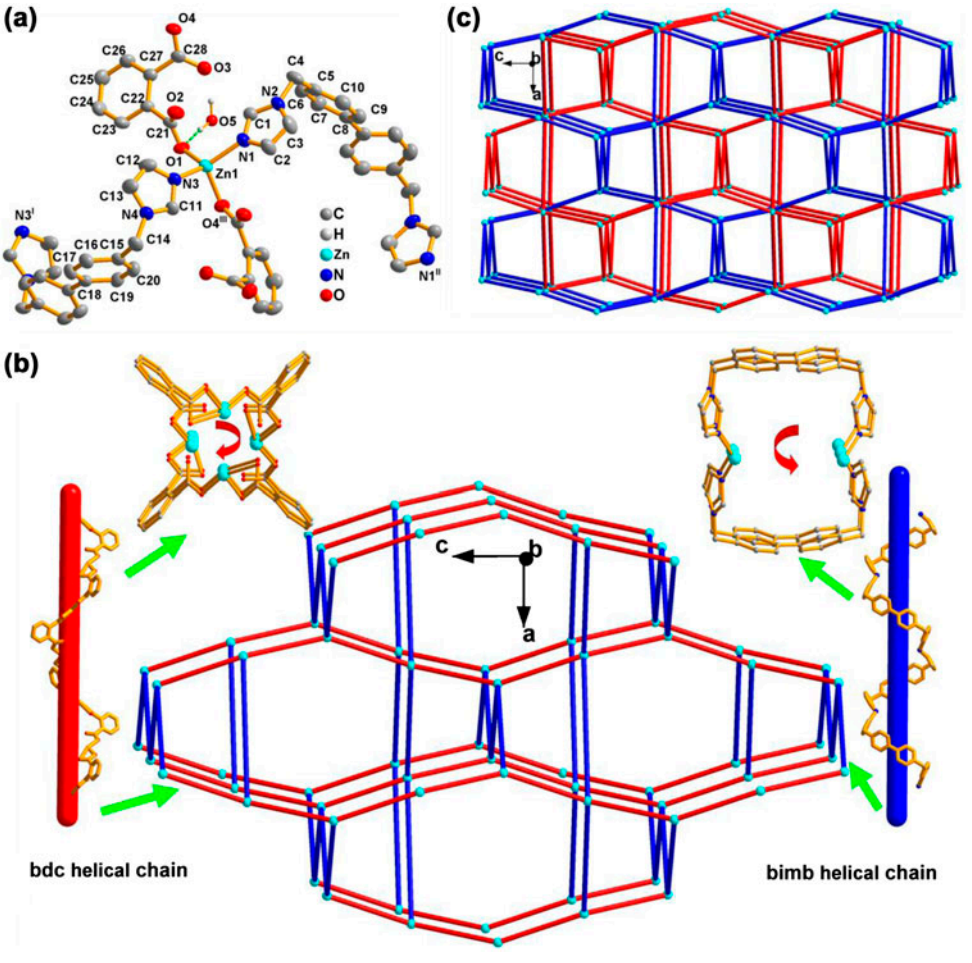

Figure 1. (a) Stick–ball representation of the structure of **1** with thermal ellipsoids at 50% probability, where hydrogens are omitted for clarity; (b) schematic illustration of 3-D four-connected **uoc** type topology with a point symbol of $(4^2{\cdot}8^4)$; (c) twofold interpenetrated **uoc** net. Symmetry codes: (I) $-x$, $0.5 - y$, z; (II) $-x$, $1.5 - y$, z; (III) $-0.25 + y$, $0.75 - x$, $-0.25 + z$.

four-coordinate in a tetrahedral environment defined by two N from two bimb molecules and two O from two bdc anions. As shown in figure 1(a), two helical chains with a same inner diameter of 6.369(1) Å along [1 0 0] and [0 1 0] directions, respectively, were formed by two bimb molecules with *cis*-conformation bridging the Zn^{II} cations. Another helical chain with a relatively small inner diameter of 2.662(1) Å along the [0 0 1] direction is built up by bdc anions linking Zn^{II} cations. The three helical chains with different rotation directions connect to construct an unusual 3-D **uoc** [11] type topology with Class IIa interpenetration and a point symbol $(4^2{\cdot}8^4)$ [figure 1(b)]. A large cavity of 12.572(2) Å × 13.643(3) Å along the [0 1 0] direction in **1** causes the occurrence of a twofold interpenetrating unusual **uoc** network with the uncoordinated water filling into the interspaces [figure 1(c)]. Such coordination networks with **uoc** twofold structures have been observed and reported very rarely. Hong [12] and Dietzel [13] reported a **uoc** twofold structure constructed by diphenic acid and 4,4′-bipyridine as mixed ligands coordinating with zinc. Similar to **1**, Zn^{II} in the

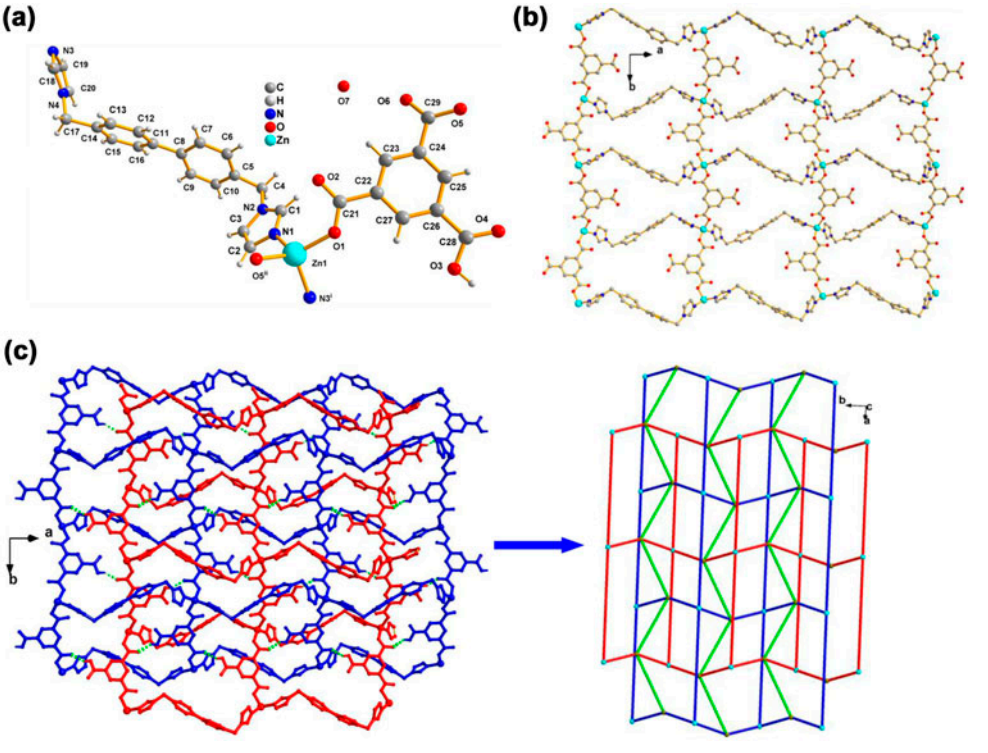

Figure 2. (a) Stick–ball representation of the structure of **2**, where hydrogens are omitted for clarity; (b) schematic illustration of 2-D **sq1** net; (c) 2-D **4,4L42** self-penetrating network with point symbol of $(5^4{\cdot}6{\cdot}8)(5^5{\cdot}6)$ when Hbtc is regarded as a four-connecting node. Symmetry codes: (I) $2+x, y, 1+z$; (II) $3-x, -0.5+y, 1.5-z$.

reported complex are also four-coordinate in a tetrahedral environment defined by two N from 4,4′-bipyridine and two O from diphenic acid. Both **1** and the reported complex are obtained from two ligands, one of which is nitrogen containing heterocyclic and the other is polycarboxylic acid, with twofold interpenetrating 3-D networks.

Complex **2** crystallizes in a monoclinic system with an asymmetric unit consisting of one bimb, one Zn^{II}, one Hbtc, and one lattice water [figure 2(a)]. The Zn^{II} is four-coordinate by two N from two bimb and two O from two Hbtc anions; the Zn–N and Zn–O distances are 1.997–2.015(2) Å. As shown in figure 2(a), bimb molecules take *trans*-conformation and connect Zn^{II} cations to form a zigzag chain along the [1 0 0] direction. Hbtc anions link adjacent chains constructing a 2-D **sq1** net with a large cavity of 10.259(2) Å × 17.209(3) Å, resulting in interpenetration similar to that in **1**. Interpenetrating **sq1** sheets are connected by hydrogen bonds O3–H3A···O2 (2.634(4) Å) of Hbtc anions to give a 2-D **4,4L42** type self-penetration network with a point symbol of $(5^4{\cdot}6{\cdot}8)(5^5{\cdot}6)$ when Hbtc is a four-connecting node. As described in a review [14], self-penetration is single network in which the smallest topological circuits are penetrated by themselves. As a kind of special interpenetration, it occured uncommonly compared with the other interpenetration structures.

Our previous investigation indicated that bimb with a long spacer could induce the formation of interpenetration structures, which could be tuned by the presence of H_2bdc as an additional ligand [15]. The aim of this study is to understand the effect of H_2bdc and H_3btc on the construction of interpenetrating frameworks. We got one 3-D network with twofold

interpenetrating structure based on H_2bdc and one 2-D self-penetrating network formed by two interpenetrating sheets connected through hydrogen bonds based on H_3btc under the same reaction conditions. In **2**, only two carboxylic groups of H_3btc coordinated with Zn^{II} because one hydrogen of carboxylic group was not deprotonated, forming hydrogen bonds to bridge two interpenetrating sheets into a self-penetration network. The structural differences between **1** and **2** could be attributed to the incomplete deprotonation of H_3btc, which provides the hydrogen bonds for two interpenetrating sheets connecting together.

3.2. *Powder X-ray diffraction and thermogravimetric analysis*

PXRD and thermogravimetric analysis (TGA) were carried out to investigate phase purities and stabilities of **1** and **2**. PXRD patterns for **1** and **2** were performed at room temperature (figure S2, ESI†). The locations and intensities of diffraction peaks of experimental patterns match well with the calculated ones, indicating that these two coordination polymers were synthesized as a single phase. TG measurements of **1** and **2** were carried out from 20 to 800 °C (figure S3, ESI†). Complex **1** shows that the first weight loss of 3.42% at 50–243 °C corresponds to loss of two lattice waters (Calcd 3.21%). The network starts to collapse at 262 °C and the second weight loss of 84.67% (Calcd 85.52%) from 262 to 502 °C can be ascribed to the removal of all bimb and bdc ligands, resulting in ZnO. For **2**, the first weight loss of 3.91% at 50–190 °C was consistent with loss of one lattice water (Calcd 2.97%). The network of **2** collapses at 327 °C, then loses 84.92% of its weight between 327 and 550 °C, corresponding to the decomposition of bimb and btc (Calcd 86.57%) with the resulting residue of ZnO. The results of PXRD and TGA are consistent with the structures of the two complexes.

3.3. *Photoluminescence properties*

The photoluminescent properties of coordination polymers, especially those with d^{10} metal centers, have been widely investigated [16], owing to their higher thermal stability than

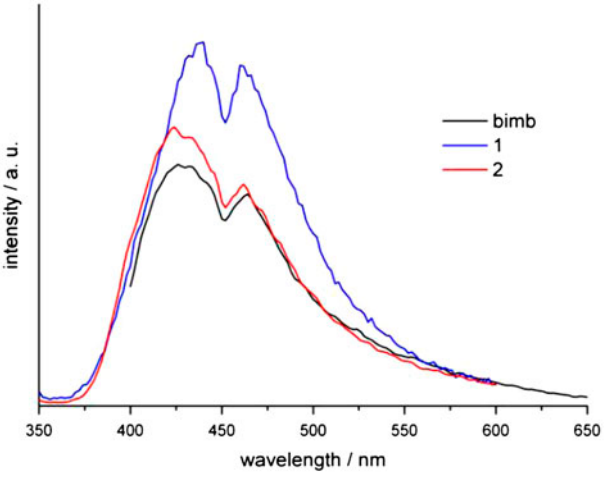

Figure 3. Solid-state photoluminescence spectra of bimb, **1** and **2**.

pure organic materials and the ability to tune the emission wavelength by metal coordination. Zinc(II) is frequently adopted for potential fluorescence-emitting coordination polymers [17]. We studied the photoluminescence properties of bimb, **1** and **2** in the solid state at room temperature. As shown in figure 3, bimb exhibits two emission bands at 428 and 464 nm ($\lambda_{ex} = 350$ nm). In **1** and **2**, since absorption spectra are similar to that of bimb, the absorption bands can be assigned to $\pi^* \rightarrow \pi$ intraligand fluorescence. Emission intensities of **1** and **2** exhibit an increase in contrast to bimb, presumably owing to the bending of ligand bonds caused by coordination.

4. Conclusion

Two coordination networks were constructed by hydrothermal reactions of zinc nitrate, bimb with H_2bdc or H_3btc. Present investigations demonstrate that a long and flexible ligand bimb tends to form structures with large cavities, favorable for the occurrence of interpenetration. Complex **1** shows a 3-D framework with twofold **uoc** interpenetration; **2** exhibits a different 2-D self-penetration network, due to hydrogen bonds of Hbtc connecting two interpenetrating **sq1** sheets. The presence of hydrogen bonds is an inducement for such a self-penetrating formation. Photoluminescence of bimb, **1,** and **2** show that the absorptions can be assigned to $\pi^* \rightarrow \pi$ intraligand fluorescence with increase of the emission intensities upon coordination.

Supplementary material

IR spectra(figure S1), PXRD patterns (figures S2) and TGA curves(figures S3) of the related compounds. Supplementary data associated with this article can be found in the online version at http://dx.doi.org/10.1080/00958972.2014.895824.

Funding

The work is financially supported by the Natural Science Foundation of Heilongjiang Province [grant number B201108]; Science and Technology Planning Project of Heilongjiang Province [grant number WJ09B03]; Scientific Research Fund of Heilongjiang Provincial Education Department [grant number 12531512].

References

[1] (a) H.K. Chae, D.Y. Siberio-Pérez, J. Kim, Y.B. Go, M. Eddaoudi, A.J. Matzger, M. O'Keeffe, O.M. Yaghi. *Nature*, **427**, 523 (2004); (b) C.L. Chen, A.M. Beatty. *J. Am. Chem. Soc.*, **130**, 17222 (2008); (c) J.W. Cheng, S.T. Zheng, W. Liu, G.Y. Yang. *CrystEngComm.*, **10**, 765 (2008); (d) X.L. Wang, H.L. Hu, G.C. Liu, H.Y. Lin, A.X. Tian. *Chem. Commun.*, **46**, 6485 (2010); (e) L. Chen, Q. Cao, L. Zhang, S.H. Gou. *J. Coord. Chem.*, **65**, 1821 (2012); (f) H.L. Jiang, T.A. Makala, H.C. Zhou. *Coord. Chem. Rev.*, **257**, 2232 (2013).
[2] S.R. Batten, R. Robson. *Angew. Chem. Int. Ed.*, **37**, 1460 (1998).
[3] S.B. Han, Z.B. Ma, Y.H. Wei, V.C. Kravtsov, B.S. Luisi, I. Kulaots, B. Moulton. *CrystEngComm.*, **13**, 4838 (2011).
[4] K. Zhou, F.L. Jiang, L. Chen, M.Y. Wu, S.Q. Zhang, J. Ma, M.C. Hong. *Chem. Commun.*, **48**, 12168 (2012).

[5] J.J. Cheng, Y.T. Chang, C.J. Wu, Y.F. Hsu, C.H. Lin, D.M. Proserpio, J.D. Chen. *CrystEngComm.*, **14**, 537 (2012).
[6] (a) T. Li, Z.H. Li, S.W. Du. *J. Coord. Chem.*, **61**, 1599 (2008); (b) G.F. Hou, X.D. Wang, Y.H. Yu, J.S. Gao, B. Wen, P.F. Yan. *CrystEngComm.*, **15**, 249 (2013); (c) B.F. Huang, H. Huang, H.P. Xiao, J.G. Wang, X.H. Li, A. Morsali. *J. Coord. Chem.*, **65**, 3605 (2012); (d) J.P. Li, H. Sun, Q.Q. Yuan, X.L. Gao, S.M. Wang, Y.Y. Zhu, L. Liu, S.H. Zhang, Y.N. Zhang, Y.X. Guo, B.X. Ye, Y.R. Liu, H.W. Hou, Y.T. Fan, J.B. Chang. *J. Coord. Chem.*, **66**, 1686 (2013).
[7] (a) L. Song, J.R. Li, P. Lin, Z.H. Li, T. Li, S.W. Du, X.T. Wu. *Inorg. Chem.*, **45**, 10155 (2006); (b) B.F. Huang, H.P. Xiao, H. Huang, X.H. Li, J.G. Wang, A. Morsali. *J. Coord. Chem.*, **66**, 904 (2013).
[8] (a) L. Carlucci, G. Ciani, S. Maggini, D.M. Proserpio. *CrystEngComm.*, **10**, 1191 (2008); (b) B.L. Fei, W.Y. Sun, Y.A. Zhang, K.B. Yu, W.X. Tang. *J. Chem. Soc., Dalton Trans.*, 2345 (2000); (c) B.Y. Li, F. Yang, Y.M. Zhang, G.H. Li, Q. Zhou, J. Hua, Z. Shi, S.H. Feng. *J. Chem. Soc., Dalton Trans.*, 2677 (2012); (d) B. Sui, W. Zhao, G. Ma, T. Okamura, J. Fan, Y.Z. Li, S.H. Tang, W.Y. Sun, N. Ueyama. *J. Mater. Chem.*, **14**, 1631 (2004).
[9] I.E. Crandall, W.A. Szarek, J.Z. Vlahakis. Patent: US2011/257235 (2011).
[10] G.M. Sheldrick. *Acta Cryst. A*, **64**, 112 (2008).
[11] (a) http://www.topos.ssu.samara.ru/authors.html; (b) V.A. Blatov. *Struct. Chem.*, **23**, 955 (2012); (c) M. O'Keeffe, M.A. Peskov, S.J. Ramsden, O.M. Yaghi. *Acc. Chem. Res.*, **41**, 1782 (2008); (d) V. Kotzabasaki, R. Inglis, M. Siczek, T. Lis, E.K. Brechin, C.J. Milios. *J. Chem. Soc., Dalton Trans.*, 1639 (2011).
[12] R.H. Wang, Y.Q. Gong, L. Han, D.Q. Yuan, M.C. Hong. *Jiegou Huaxue*, **24**, 1007 (2005).
[13] P.D.C. Dietzel, R. Blom, H. Fjellvag. *Dalton Trans.*, 586 (2006).
[14] S.R. Batten. *CrystEngComm.*, **3**, 67 (2001).
[15] G.F. Hou, B. Wen, Y.H. Yu, J.S. Gao, X.D. Wang, P.F. Yan. *Inorg. Chim. Acta*, **402**, 128 (2013).
[16] (a) M.L. Tong, X.M. Chen, B.H. Ye, L.N. Ji. *Angew. Chem., Int. Ed.*, **38**, 2237 (1999); (b) X.L. Wang, C. Qin, E.B. Wang, L. Xu, Z.M. Su, C.W. Hu. *Angew. Chem., Int. Ed.*, **43**, 5036 (2004); (c) X.M. Zhang, M.L. Tong, M.L. Gong, X.M. Chen. *Eur. J. Inorg. Chem.*, **138**, 2237 (2003).
[17] (a) L.L. Wen, D.B. Dang, C.Y. Duan, Y.Z. Li, Z.F. Tian, Q.J. Meng. *Inorg. Chem.*, **44**, 7161 (2005); (b) G.H. Wei, J. Yang, J.F. Ma, Y.Y. Liu, S.L. Li, L.P. Zhang. *J. Chem. Soc., Dalton Trans.*, 3080 (2008); (c) F. Guo. *J. Coord. Chem.*, **43**, 621 (2013); (d) X. Feng, L. Liu, J.G. Zhou, L.L. Zhou, Z.Q. Shi, L.Y. Wang. *J. Coord. Chem.*, **43**, 705 (2013).